

and our analysis is entirely consistent with the ground-state term assignment ${}^4E_g(e_g^3a_{1g}b_{2g})$. This conclusion is in disagreement with the results of magnetic measurements on the β -phase solid¹³⁻¹⁷ which suggest a ${}^4A_{2g}(b_{2g}^2e_g^2a_{1g})$ ground-state term. The difference may be due to the fact that azamethine nitrogens of adjacent molecules lie above and below the Mn atoms in the β -phase.^{21,22}

The dispersion of the MCD bands and correlations with earlier electrochemical data^{10,34} have allowed us to formally assign the major bands in the electronic spectra. We are confident of our ability to distinguish between transitions that are principally of $\pi \rightarrow \pi^*$ or CT character, but more specific descriptions await a sophisticated quantum-mechanical calculation for both the ground and excited states.

The absorption spectrum of MnPc/Ar is quite different from

earlier solution spectra,^{3-5,8-11} a fact that may be attributable to axial ligation (with oxygen in some cases) and perhaps to a difference in ground state. Our results suggest that the strongest red band of the solution spectra contains contributions from both the $Q(\pi \rightarrow \pi^*)$ and LMCT1 excitations.

Acknowledgment. This work was supported by the National Science Foundation under Grants CHE8700754 and CHE8902456 and by the Natural Sciences and Engineering Research Council of Canada (to M.J.S.). One of us (M.E.B.) acknowledges partial support from the ONT/NRL Laser Block Program. We acknowledge the assistance of Z. Gasyana and R. J. Van Hale with some of the experimental work.

Registry No. MnPc, 14325-24-7.

Pentaenyl Cations from the Photolysis of Retinyl Acetate. Solvent Effects on the Leaving Group Ability and Relative Nucleophilicities: An Unequivocal and Quantitative Demonstration of the Importance of Hydrogen Bonding

Norbert J. Pienta* and Robert J. Kessler

Contribution from the Department of Chemistry, CB # 3290, University of North Carolina, Chapel Hill, North Carolina 27599-3290. Received June 12, 1991

Abstract: The photolysis of retinyl acetate leads to carbon-oxygen bond heterolysis and yields the retinyl cation within 100 ps. This pentaenyl cation, which has an absorbance centered at 590 nm, is observed using picosecond and nanosecond laser transient absorption. This provides access to ion dynamics and affords the opportunity to study aspects of the S_N1 mechanism, including the effect of hydrogen bonding cosolvents like water and alcohols. Contact ion pairs appear to be important in the early time regime, but free ions are the reactive species in polar solvents in the nanosecond experiment. Trapping of the free ions with nucleophiles yields a collection of rate data from Stern-Volmer quenching which in turn gives linear plots versus Pearson/Swain-Scott n values, measures of relative nucleophilicity based on S_N2 reactions. These linear plots show a marked dependence on water content in the solvent acetonitrile with an increase in selectivity (i.e., slope of the line) with added water. For example, the second order rate constant for reaction of the retinyl cation with fluoride decreases by over four orders of magnitude in changing the solvent from dry acetonitrile to the same solvent with 11 M water. This is interpreted to be the result of hydrogen bonding between water and the nucleophiles. The special salt effect of Li^+ is also demonstrated to arise from the strong interaction of this Lewis acid and the nucleophiles.

Introduction

Reactions of carbenium ions with nucleophiles have been studied extensively, and recent work includes the use of laser flash photolysis to measure rate constants directly.¹ Other sources of absolute rate constants come from reactions of very stable cations

using rapid mixing techniques and include studies by Ritchie² and Bunton.³ A comprehensive picture is beginning to emerge and, for example, includes models for the relationship between solvolytic reactivity and nucleophile selectivity⁴ and for the coordination of carbanions with carbenium ions.⁵ In spite of these efforts and despite implications of the importance of hydrogen bonding,^{1a,6,7}

(1) (a) McClelland, R. A.; Kanagasabapathy, V. M.; Banait, N. S.; Steenken, S. *J. Am. Chem. Soc.* **1991**, *113*, 1009-14. (b) McClelland, R. A.; Banait, N. S.; Steenken, S. *J. Am. Chem. Soc.* **1989**, *111*, 2929-35. (c) *J. Am. Chem. Soc.* **1986**, *108*, 7023-27. (d) McClelland, R. A.; Kanagasabapathy, V. M.; Steenken, S. *J. Am. Chem. Soc.* **1988**, *110*, 6913-4. (e) McClelland, R. A.; Kanagasabapathy, V. M.; Banait, N. S.; Steenken, S. *J. Am. Chem. Soc.* **1989**, *111*, 3966-72. (f) Steenken, S.; McClelland, R. A. *J. Am. Chem. Soc.* **1989**, *111*, 4967-73. (g) Faria, J. L.; Steenken, S. *J. Am. Chem. Soc.* **1990**, *112*, 1277-9. (h) McClelland, R. A.; Mithavanan, N.; Steenken, S. *J. Am. Chem. Soc.* **1990**, *112*, 4857-61. (i) Bartl, J.; Steenken, S.; Mayr, H.; McClelland, R. A. *J. Am. Chem. Soc.* **1990**, *112*, 6918-28. (j) McClelland, R. A.; Cozens, F.; Steenken, S. *Tetrahedron Lett.* **1990**, 2821-24. (k) Schnabel, W.; Naito, I.; Kitamura, T.; Kobayashi, S.; Taniguchi, H. *Tetrahedron* **1980**, *36*, 3229-31. (l) Kobayashi, S.; Kitamura, T.; Taniguchi, H.; Schnabel, W. *Chem. Lett.* **1983**, 1117-20. (m) Van Ginkel, F. I. M.; Visser, R. J.; Varma, C. A. G. O.; Lodder, G. *J. Photochem.* **1985**, *30*, 453-73. (n) Kobayashi, S.; Zhu, Q. Q.; Schnabel, W. *Z. Naturforsch.* **1988**, *43B*, 825-9. (o) Minto, R. E.; Das, P. K. *J. Am. Chem. Soc.* **1989**, *111*, 8858-66. (p) Johnston, L. J.; Lobaugh, J.; Wintgens, V. *J. Phys. Chem.* **1989**, *93*, 7370-4. (q) Alonso, E. O.; Johnston, L. J.; Scatano, J. C.; Toscano, V. G. *J. Am. Chem. Soc.* **1990**, *112*, 1270-1.

(2) (a) Ritchie, C. D. In *Nucleophilicity*; Harris, J. M., McManus, S. P., Eds.; Advances in Chemistry Series 215; American Chemical Society: Washington, DC, 1987; pp 169-79. (b) Ritchie, C. D.; Hofelich, T. C. *J. Am. Chem. Soc.* **1980**, *102*, 7039-44. (c) Ritchie, C. D.; Gandler, J.; *J. Am. Chem. Soc.* **1979**, *101*, 7318-23. (d) Ritchie, C. D. *Acc. Chem. Res.* **1972**, *5*, 348-54, and references cited therein.

(3) (a) Bunton, C. A.; Paik, C. H. *J. Org. Chem.* **1976**, *41*, 40-4. (b) Bunton, C. A.; Huang, S. K. *J. Am. Chem. Soc.* **1973**, *95*, 2701-2. (c) *J. Am. Chem. Soc.* **1974**, *96*, 515-22; **1972**, *94*, 3536-44.

(4) Ta-Shma, R.; Rappoport, Z. *J. Am. Chem. Soc.* **1983**, *105*, 6082-95.

(5) (a) Arnett, E. M.; Amarnath, K.; Harvey, N. G.; Cheng, J. P. *J. Am. Chem. Soc.* **1990**, *112*, 344-55. (b) Arnett, E. M.; Molter, K. E. *Acc. Chem. Res.* **1985**, *18*, 339-46, and references cited therein.

(6) (a) Reichardt, Chr. *Solvents and Solvent Effects in Organic Chemistry*, 2nd ed.; VCH: New York, 1990, pp 208-283, and references cited therein. (b) Epshtein, E. P. *Russian Chem. Rev.* **1979**, *48*, 854. (c) Okamoto, K. *Pure Appl. Chem.* **1984**, *56*, 1797. (d) Parker, A. J. *Chem. Soc. Quart. Rev.* **1962**, *16*, 163. (e) Parker, A. J. *Adv. Phys. Org. Chem.* **1968**, *5*, 173-235.

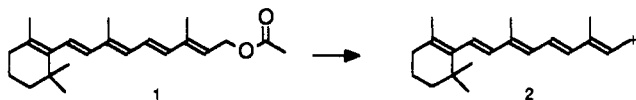
Table I. Second Order Rate Constants for Reaction of Nucleophiles with **2** in CH₃CN

Nu =	<i>n</i> _{MeI} ^a	<i>k</i> , M ⁻¹ s ⁻¹				ΔΔ <i>G</i> ^{‡c}
		dry ^b	1 M H ₂ O	11 M H ₂ O	36 M H ₂ O	
1. H ₂ O	(-1.0) ^d				1.0 × 10 ²	
2. CF ₃ SO ₃ ⁻				<10 ²		
3. CH ₃ OH	0.0			(1.1 × 10 ³) ^e	(1.1 × 10 ³) ^e	
4. <i>p</i> -MePhSO ₃ ⁻		1.2 × 10 ⁸		2.2 × 10 ⁴		5.01
5. NO ₃ ⁻	1.5	1.8 × 10 ⁷	1.2 × 10 ⁶	4.1 × 10 ⁴	1.4 × 10 ⁴	3.54
6. F ⁻	2.7	1.1 × 10 ⁹	1.4 × 10 ⁷	6.1 × 10 ⁴		5.70
7. OAc ⁻	4.3	5.1 × 10 ⁹	1.6 × 10 ⁸	3.8 × 10 ⁵		5.53
8. Cl ⁻	4.37	2.6 × 10 ⁹	3.3 × 10 ⁷	1.9 × 10 ⁶		4.20
9. Br ⁻	5.79	1.4 × 10 ⁹	1.1 × 10 ⁸	1.9 × 10 ⁶		3.84
10. N ₃ ⁻	5.78			1.1 × 10 ⁷		
11. SCN ⁻	6.7			1.9 × 10 ⁷		2.71
12. (CH ₃ CH ₂) ₃ N	6.66			3.0 × 10 ⁷		
13. (Ph) ₃ P	7.0			7.4 × 10 ⁷		
14. I ⁻	7.42	4.0 × 10 ⁹	7.7 × 10 ⁸	9.2 × 10 ⁷		2.20
15. PhS ⁻	9.92					

^aPearson *n* values (ref 17). ^bHPLC grade CH₃CN to which no water was intentionally added (see Experimental Section). ^cCalculated from ΔΔ*G*[‡] (kcal/mol) = 2.3RT log *k*₁/*k*₂ with 2.3RT = 1.34 kcal/mol, using *T* = 295 K, the rate in CH₃CN as *k*₁ and the rate in 11 M water as *k*₂. ^dEstimated, this work. ^eFrom high concentration of CH₃OH region (16–24.7 M).

there has been no systematic study of the nature and magnitude of hydrogen bonding effects on the coordination of carbenium ions with nucleophiles. This work will provide unequivocal evidence for the importance of hydrogen bonding on leaving group ability and on nucleophilicity.

Photolysis and pulsed radiolysis of retinol and retinyl acetate **1** lead to heterolysis of the C–O bond⁸ and afford the opportunity to study ion dynamics from tens of picoseconds to seconds.^{9,10} The rapid bond fragmentation enables one to enter the reaction coordinate at the earliest stages (when the ions are presumably in the form of contact ion pairs) and to follow the course to its completion, thereby providing a complete temporal picture of the ubiquitous S_N1 reaction. The precursor **1** is ideally suited to these



studies since the chromophore (maximum at ca. 340 nm) is accessible to a convenient laser excitation wavelength (355 nm), and the cation absorbs in the visible (maximum at ca. 590 nm) with a large extinction coefficient (ca. 10⁴) and no overlapping interferences. We will attempt to convince the reader here and in subsequent reports that cation **2** is not exceptional but is in fact representative of this entire class of intermediates.

Experimental Section

General. The precursor, *all-trans*-retinyl acetate **1**, is commercially available (Sigma) and was used as obtained. Less than 0.2% of retinol

(7) (a) Jencks, W. P. In *Nucleophilicity*; Harris, J. M., McManus, S. P., Eds.; Advances in Chemistry Series 215; American Chemical Society: Washington, DC, 1987; pp 155–67. (b) Jencks, W. P. *Chem. Soc. Rev.* **1981**, 10, 345–75. (c) Jencks, W. P. *Acc. Chem. Res.* **1980**, 13, 161–9, and references cited therein. (d) Richard, J. P. *J. Chem. Soc., Chem. Commun.* **1987**, 1768–9.

(8) (a) Bhattacharyya, K.; Rajadurai, S.; Das, P. K. *Tetrahedron* **1987**, 43, 1701–11. (b) Bobrowski, K.; Das, P. K. *J. Am. Chem. Soc.* **1982**, 104, 1704–9. (c) Chattopadhyay, S. K.; Bobrowski, K.; Das, P. K. *Chem. Phys. Lett.* **1982**, 91, 143. (d) Lo, K. K. N.; Land, E. J.; Truscott, T. G. *Photochem. Photobiol.* **1982**, 36, 139. (e) Rosenfeld, T.; Alchalal, A.; Ottolenghi, M. *Chem. Phys. Lett.* **1973**, 20, 291. (f) Rosenfeld, T.; Alchalal, A.; Ottolenghi, M. In *Excited States of Biological Molecules*; Birks, J. B., Ed.; Wiley: New York, 1976; pp 540–54.

(9) For studies of ion pairs generated by electron transfer on the picosecond time scale, see: (a) Peters, K. S. *Ann. Rev. Phys. Chem.* **1987**, 38, 253–70. (b) Masnovi, J. M.; Kochi, J. K. *J. Am. Chem. Soc.* **1985**, 107, 7880–93. (c) Simon, J. D.; Peters, K. S. *Acc. Chem. Res.* **1984**, 17, 277–83.

(10) The studies of the photochemistry of **1** by steady irradiation include quantum yields for substitution, elimination, and *cis*–*trans* isomerization reactions: Pienta, N. J.; Culp, S. J.; Judy, S.; Durham, B., manuscript in preparation. Preliminary results have been reported: (a) Pienta, N. J.; Culp, S. J.; Durham, B.; Johnson, D. A. 193rd National Meeting of the American Chemical Society, Denver, CO: April 1987. (b) Culp, S. J. Ph.D. Dissertation, University of Arkansas, 1987.

and 0.3% of other geometric isomers of **1** were detected by HPLC (250 × 4.6 mm ODS column with 5 μm particles; elution with 90:10 acetonitrile/water; UV-visible diode array detection). Anionic nucleophiles (except the azide) were commercially obtained as tetrabutylammonium TBA salts (Aldrich) and used without purification. The salts were stored under vacuum in a desiccator containing drying agent. TBA⁺N₃⁻ was prepared from NaN₃ and TBA⁺HSO₄⁻ (Aldrich) according to an available procedure.¹¹ Lithium perchlorate (Alfa) and tetrafluoroborate (Alfa) were stored in vacuo and used as obtained. All organic solvents were HPLC grade and were used as obtained. Dry acetonitrile generally came from freshly opened bottles.

Picosecond Transient Absorption. Spectra were obtained with the help and guidance of K. S. Peters and E. D. O'Driscoll at the University of Colorado. A description of the instrumentation has been given.¹² Solutions of **1** were prepared so that the optical density at 355 nm, the irradiation wavelength, was just greater than 2.0 (0.1–0.2 mM). These solutions were then passed through a 1 × 1 cm flow cell using a syringe pump (0.2–0.6 mL/min) and subjected to irradiation. The laser was operated at 1 Hz, and 500 repetitions were collected and averaged. Observation times were changed by moving a mirror on a micrometer stage and/or with fiber-optic delay lines. (Delay lines corresponding to 0, 300, 600, 750, and 900 ps and 1.65, 3, and 9 ns were available; micrometer translation was capable of continuously adjusting the delay from ca. 0 to 400 ps.) The probe light, provided by the continuum generated by 50:50 H₂O/D₂O, was limited to the range ca. 420–630 nm by the configuration used. (Little or no probe light intensity was available outside that range.) The ca. 200-nm spectral region was collected and stored digitally as OD, and the spectra represent ca. 350 points each. Sufficient spectra (i.e., at 7–12 different times) were obtained under each set of reaction conditions. A plot of log (ΔOD at 590 nm) versus time for this limited number of points does not appear to be linear.

The photodissociation of retinol has been reported to be biphotonic.⁸ As a result, we measured the yield of cation from a solution of **1** in CH₃CN as a function of irradiating pulse intensity. Thus, a spectrum was collected in the usual way, and the OD was recorded. Then a series of neutral density filters of known transmittance were placed in the path of the pulse (i.e., 355 nm) beam, and the spectrum was collected again. They yield the following data (%T of 355 nm beam, OD of 590 nm transient): 100% T, 0.42 OD; 84.4% T, 0.38 OD; 47.8% T, 0.21 OD; 31.6% T, 0.10 OD. The slope is linear and suggests only one photon is required per cation formed.

Nanosecond Transient Absorption. Absorption data were collected with an apparatus that has been described previously.¹³ Samples in this study were irradiated with the third harmonic of the Nd⁺/YAG at 355 nm parallel to the probe beam, a Xe arc lamp. The probe was generally flashed except when analysis times greater than 200 μs were required, in which case the arc was on continuously but impinged on the sample only when an electronically controlled shutter was opened.

Samples for Stern–Volmer quenching were prepared by making a

(11) Brandstrom, A.; Lamm, B.; Palmertz, I. *Acta Chem. Scand. B* **1974**, 28, 699.

(12) Simon, J. S.; Peters, K. S. *J. Am. Chem. Soc.* **1981**, 103, 6403. (b) O'Driscoll, E. D. Ph.D. Dissertation, University of Colorado, 1989.

(13) Boyde, S. L.; Strouse, G. F.; Jones, W. E.; Meyer, T. J. *J. Am. Chem. Soc.* **1989**, 111, 7448–54.

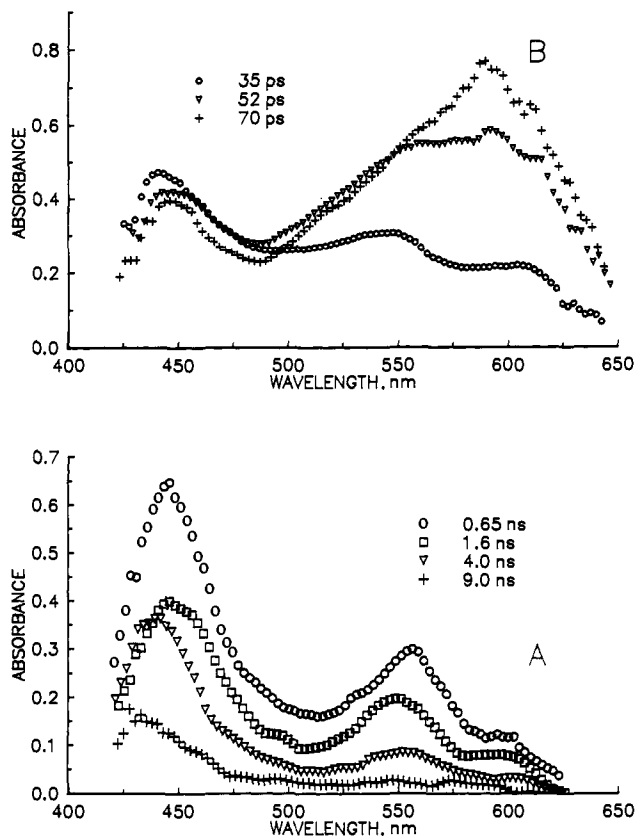


Figure 1. Picosecond transient absorption spectra from irradiation of **1**: in hexane (A) and in CH₃CN (B).

stock solution of 0.05–0.1 mM **1** in the indicated solvent. Nucleophile was added by (a) weighing an appropriate amount of solid TBA salt into a glass test tube (13 × 100 nm) and filling with 5.0 mL of the precursor stock solution (using a Brinkmann Dispensette) or (b) preparing a nucleophile stock solution with weighed solid and 5 mL of precursor stock and adding 5–100 μ L of the nucleophile stock to 5 mL of the precursor stock in the test tube. The test tubes were sealed with Parafilm, stirred with a vortex stirrer, and used directly in the sample compartment of the laser. Samples were generally freshly prepared just prior to use, but control experiments show that there is no discernible ground state reaction at room temperature for days.

Each of the samples described above was irradiated at 355 nm and monitored at 590 nm. The intensity measured with the laser on and off are each the average of 10 pulse-probe sequences, and the decays each contain 500–2000 points, depending on the duration of the analysis. Nonlinear least squares analyses were performed using a Gauss gradient search algorithm for nonlinear regression adapted from a public domain routine (D. Whitman, Cornell University) to DOS-based 386 microcomputers by FK Enterprises (Chapel Hill). The fits give rate constants with $\pm 10\%$ standard deviations. The samples were maintained at 22 ± 1 °C.

In the absence of added nucleophiles, the cation absorbance decay is second order (i.e., $[2] = [\text{OAc}^-] = \text{ca. } 20 \mu\text{M}$), and the rate constant is calculated in units of $\text{M}^{-1} \text{s}^{-1} \epsilon^{-1}$. It can be converted to a true second order rate by multiplying with the extinction coefficient for **2** at 590 nm in CH₃CN, $3.6 \times 10^3 \text{ M}^{-1} \text{ cm}^{-1}$. (The extinction coefficient was measured by titrating CF₃CO₂H in CH₃CN into a 0 °C solution of **1** in CH₃CN.¹⁰ Alternatively, a similar value is obtained by dividing the true second order rate constant for reaction of acetate with **2** from Table I ($5.1 \times 10^9 \text{ M}^{-1} \text{ s}^{-1}$) by the second order rate for acetate and **2** recombination in the absence of any added nucleophile that is obtained directly from the fits ($6.3 \times 10^5 \text{ M}^{-1} \text{ s}^{-1} \epsilon^{-1}$.) In the presence of nucleophiles, the pseudo-first-order decay rate measured, k_{obs} , was determined as a function of the concentration of an added nucleophile (i.e., typical Stern–Volmer quenching) and used to determine the second order rate constants (see Figure 6). Generally, 7–10 concentrations of nucleophiles were chosen so that the observed rate changed by a factor of 5–10, and the slope of the least squares line gave the second order rate constant directly. (The standard deviations of the slopes were ± 5 –15%.) Those second order rates are given in Table I.

The spectrum in Figure 3 was obtained by measuring the decay at each of the indicated wavelengths and plotting the recorded OD at the indicated times.

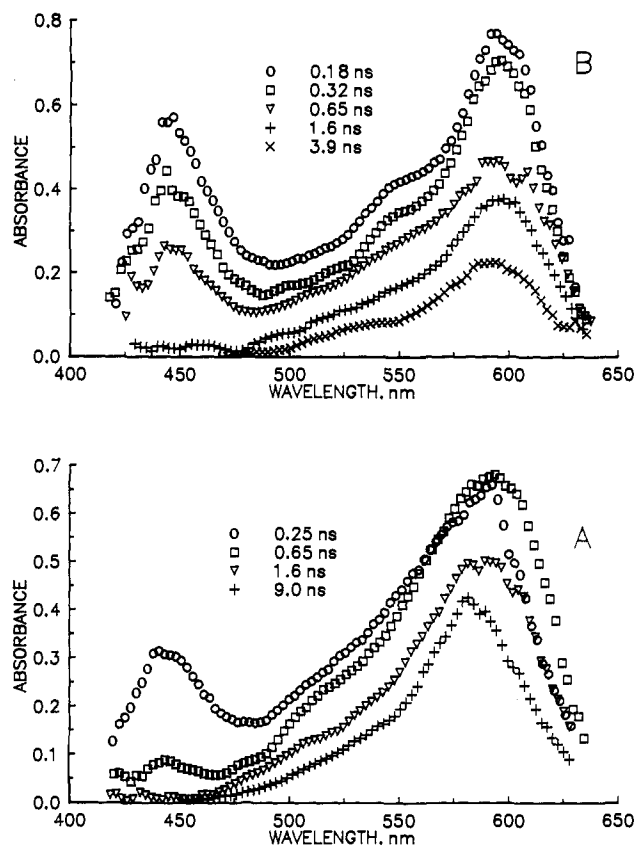


Figure 2. Picosecond transient absorption spectra from irradiation of **1**: in CH₃CN (A) and in CH₂Cl₂ (B).

Results

Spectra of Transients. Figure 1 shows typical picosecond spectra from (A) the irradiation of **1** in hexane in which peaks are observed at ca. 450 and 550 nm and (B) from early times in acetonitrile in which an additional feature grows in at ca. 590 nm. Figure 2 contains spectra from the irradiation of **1** in CH₃CN (A) and CH₂Cl₂ (B) at later times that demonstrate the disappearance of the various spectral features. The peaks in hexane (Figure 1A) both apparently decay at the same rate (based on the data in the literature⁸ which is more suitable for kinetic analysis), and appear to give rise to the additional peak at 590 nm when the solvent is changed to a more polar one (e.g., see Figure 1B). Thus, the peaks at ca. 450 and 550 nm are assigned to the singlet excited state of **1** and have decays that are consistent with fluorescence lifetimes (4.8, 2.85, 1.37, and 0.80 ns in hexane, 1-butanol, ethanol, and methanol, respectively) reported in the literature.^{8f} The shorter lifetime of the singlet excited state of **1** in polar solvents is consistent with the addition of another pathway for its decay and thus supports the suggestion that the singlet (i.e., ca. 450 and 550 nm peaks) is the precursor to the peak at 590 nm.

In the picosecond experiment, the cation **2** is apparent in polar solvents from the earliest times shown (ca. 35 ps) until the longest measured one (ca. 9 ns). Once the cation **2** peak has grown in, virtually no changes are detectable except perhaps a narrowing of the 590 nm peak and/or a shift to shorter wavelengths (e.g., in the ns range of the picosecond experiment in Figure 2). The decay of the 590-nm peak appears to be somewhat solvent dependent with the disappearance faster in CH₂Cl₂ than in CH₃CN.

A spectrum from the irradiation of **1** in CH₃CN was obtained using the nanosecond instrumentation and is shown in Figure 3. The spectral feature at 590 nm persists from the picosecond time scale long past the duration of the nanosecond experiment shown (ca. 5 μ s). The singlet excited state (peaks at ca. 450 and 550 nm) is long gone. A new peak at 400 nm has grown in and decays in the time shown and is assigned to the triplet excited state.^{8c–f,14,15}

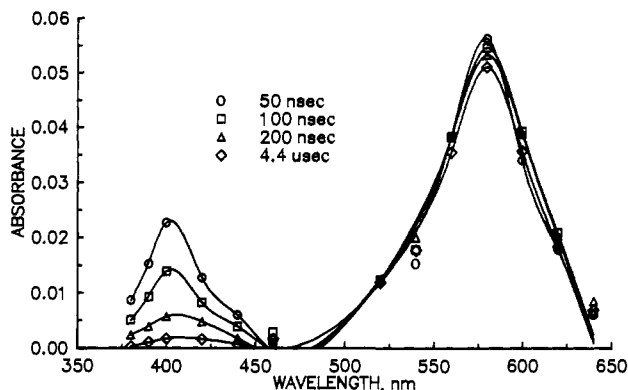


Figure 3. Nanosecond transient absorption spectra from irradiation of **1** in CH_3CN .

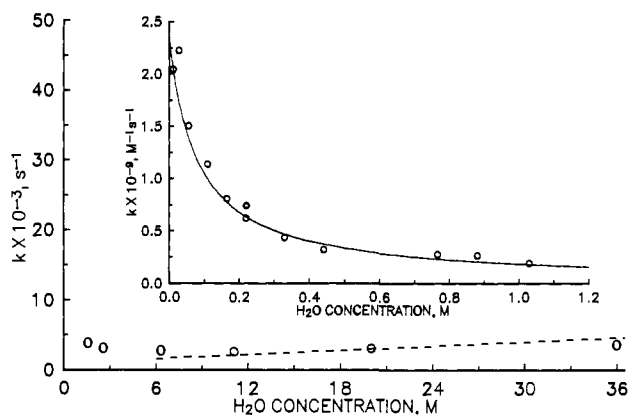


Figure 4. Observed decay from irradiation of **1** in CH_3CN /water mixtures versus the water concentration. The inset contains a plot of the second order rate constants versus $[\text{H}_2\text{O}]$, and the line through the points is a fit in which recombination of acetate and **2** is being effected by the addition of water with $K = 25$ (see eq 4 and text). The dashed line is the fit to the points from a plot of pseudo-first-order rate constants in which water adds to **2**. The slope of the dashed line (ca. $100 \text{ M}^{-1} \text{ s}^{-1}$) is the second order rate constant reported in Table I.

Stern–Volmer Quenching. The data in Figures 4 and 5 show that alcohols and water produces *negative, nonlinear* Stern–Volmer effects (i.e., a decrease in rate of disappearance of the cation with increasing hydroxylic solvent concentration). However, water and the alcohols do behave as nucleophiles under the appropriate conditions, and that can be seen at the highest concentrations, where positive Stern–Volmer regions are apparent. For example, in Figure 5 two regions with positive slopes start at concentrations of methanol and 2-propanol greater than ca. 2–3 M and proceed through the highest percentages of alcohol. (Note that the last point for both methanol and 2-propanol corresponds to 100% alcohol.) The linear portion of the water data is not quite as obvious (see Figure 4, dashed line).

Figure 6 shows that Li^+ (added as the perchlorate or tetrafluoroborate salts, see Experimental Section) produces the same kind of effect, although much smaller concentrations of it are necessary to reach an asymptote. There is greater scatter in the data presumably because of the difficulty in accurately preparing solutions of such low concentrations. The flat line in Figure 6 comes from $\text{TBA}^+\text{BF}_4^-$ and shows the negligible effect of ionic strength (i.e., from a nonnucleophilic anion and a noninteracting cation) in this concentration range.

(14) Sykes, A.; Truscott, T. G. *J. Chem. Soc., Chem. Commun.* **1969**, 929.

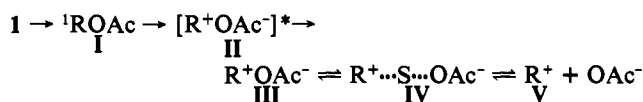
(15) The peak at 400 nm in Figure 3 decays at $2.8 \times 10^6 \text{ s}^{-1}$ in N_2 saturated CH_3CN and at $8.6 \times 10^6 \text{ s}^{-1}$ in air saturated CH_3CN . This corresponds to a diffusion controlled rate if one assumes an O_2 concentration of ca. 0.4 mM: Clever, H. L.; Battino, R. In *Techniques of Chemistry: Solutions and Solubilities*; Dack, M. R. J., Ed.; Wiley: New York, Vol. VIII, Part I, pp 380–414.

Data obtained from the addition of acetate OAc^- to **2** in dry CH_3CN are shown in Figure 7 and are representative of the nucleophiles (vide supra).¹⁶ The inset to Figure 7 shows an actual decay (from $[\text{OAc}^-] = 200 \mu\text{M}$) and the single exponential fit to it ($k = 1.1 \times 10^6 \text{ s}^{-1}$). Such a line was obtained for each nucleophile under the solvent conditions employed. Thus, the effect of solvent water content on the rates of reaction of a variety of nucleophiles can be seen in Table I and Figure 8. Table I contains the second order rate constants obtained from the linear plots (like that shown in Figure 7). They were determined in CH_3CN or CH_3CN with 1, 11, or 36 M H_2O as the cosolvent. Figure 8 contains the data from Table I plotted with the log of the second order rate constants as the ordinate and Pearson/Swain–Scott n values¹⁷ as the abscissa. These plots appear to be quite linear over seven orders of magnitude of $\log k$ in the ordinate and ca. ten orders of magnitude of relative nucleophilicity in the abscissa. The least squares lines are drawn through the three plots, and all appear to intersect at $k = 5 \times 10^9 \text{ M}^{-1} \text{ s}^{-1}$ ($\log k = 9.7$), which is near the diffusion controlled rate in CH_3CN and at the approximate value of the most reactive nucleophile (i.e., PhS^- at $n = 9.92$). Somewhat higher diffusion controlled limits (i.e., $2 \times 10^{10} \text{ M}^{-1} \text{ s}^{-1}$) have been reported by McClelland et al. during coordination reactions between carbonium ions and anions in similar solvents, and the larger rates ascribed to an enhancement due to coulombic attraction when anionic nucleophiles are used.¹⁸ Some of their data are plotted in Figure 10, and it is interesting to note that the fastest rate (azide, $4 \times 10^9 \text{ M}^{-1} \text{ s}^{-1}$) appears to be “exceptional” in that it does not fit the line through the other points. (See later discussions.)

Discussion

The Nature of the Cation. The irradiation of **1** in CH_3CN on the picosecond time scale leads to formation of transients that include a peak at 590 nm, which has been assigned to **2**.⁸ The intermediate **2** has been generated previously by the action of strong acids on solutions of retinol and **1** in organic solvents.¹⁸ The absorption maximum is consistent with maxima of other pentaenyl cations¹⁹ or as part of a series of conjugated systems studied by Sorensen.²⁰

Photolysis of **1** in solvents of at least moderate polarity leads to formation of the retinyl cation **2** at the earliest detection time (ca. 25 ps), and some form of the cation persists until milliseconds or longer, depending on the conditions. We suggest a sequence of events that in its latter stages is identical to ion dynamics from thermal reactions (i.e., $\text{S}_{\text{N}}1$):



Irradiation of **1** leads to the singlet excited state **I** and is followed by C–O bond heterolysis. Intermediate **II** represents a contact ion pair which contains excess vibrational energy that is lost to the solvent microenvironment early on the picosecond time scale.²¹ From this point on, the mechanism is identical to one typically drawn for the $\text{S}_{\text{N}}1$ reaction. Cation **2** can be any or all of the kinetic forms of the cation: **III**, the contact ion pair; **IV**, the solvent

(16) With added nucleophiles at concentrations considerably greater than the concentration of cation **2** ($[\text{Nu}] \gg [\text{2}] = \text{ca. } 20 \mu\text{M}$), one observes pseudo-first-order kinetics. In the absence of such rate enhancements, the observed decay is second order, and the determination of a true second order rate constant requires the extinction coefficient of **2**.

(17) Pearson, R. G.; Sobel, H.; Songstad, J. *J. Am. Chem. Soc.* **1968**, *90*, 319–26. (b) Swain, C. G.; Scott, C. B. *J. Am. Chem. Soc.* **1953**, *75*, 171.

(18) Baltz, P. E.; Pippert, D. L. *J. Am. Chem. Soc.* **1968**, *90*, 1296.

(19) Olah, G. A.; Pittman, C. U., Jr.; Symons, M. C. R. In *Carbonium Ions*; Olah, G. A.; Schleyer, P. v. R., Eds.; Interscience: New York, Vol. I, pp 155–222.

(20) Sorensen, T. S. *J. Am. Chem. Soc.* **1965**, *87*, 5075.

(21) For discussions on solvent reorganization following ion formation on the picosecond time scale, see: (a) Castner, E. W., Jr.; Maroncelli, M.; Fleming, G. R. *J. Chem. Phys.* **1987**, *86*, 1090–97. (b) Kosower, E. M. *J. Am. Chem. Soc.* **1985**, *107*, 1114–8. (c) Simon, J. D.; Peters, K. S. *J. Am. Chem. Soc.* **1981**, *103*, 6403–6.

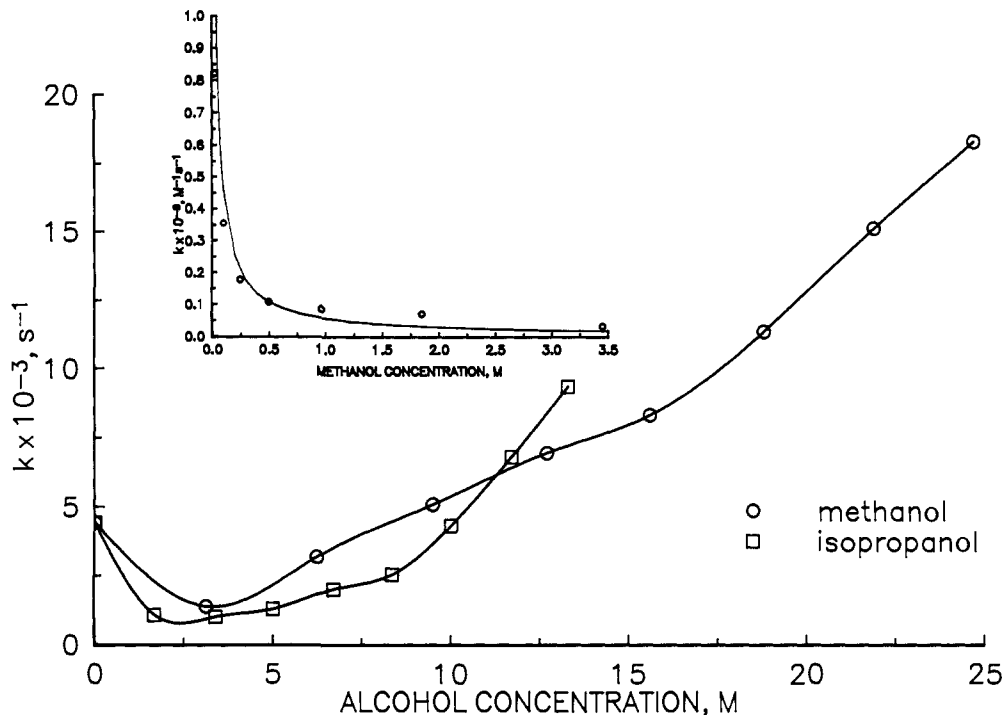


Figure 5. Observed rate from the irradiation of **1** in CH_3CN /alcohol mixtures versus the concentration of the alcohol: methanol (circles) and 2-propanol (squares). The inset contains a plot of the second order rate constants versus $[\text{MeOH}]$, and the line through the points is a fit in which recombination of acetate and **2** is being effected by the addition of the methanol with $K = 25$ (see eq 4 and text).

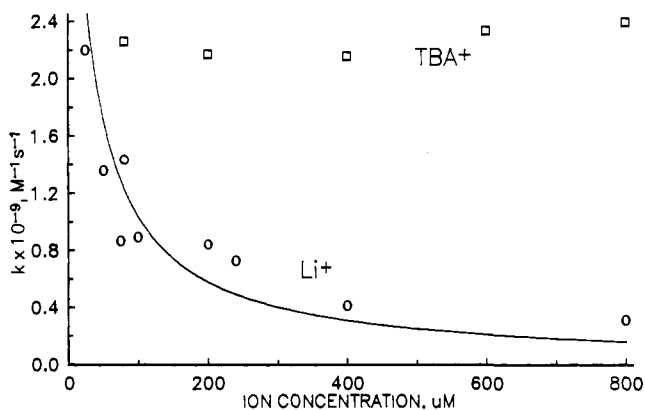


Figure 6. Observed rate from the irradiation of **1** in CH_3CN versus the concentration of added ions: Li^+BF_4^- or $\text{Li}^+\text{ClO}_4^-$ (circles) and tetrabutylammonium $\text{TBA}^+\text{BF}_4^-$ (squares). The fit line is from eq 4 (see text).

separated ion pair;²² or **V**, the free ions. These three forms are not discernible from their visible spectra, and indeed we expect that they are all present at various stages in the picosecond data.

In a nonpolar solvent like hexane (Figure 1A), irradiation of **1** leads to the singlet excited state **I** which decays via the usual radiative and nonradiative channels. Both peaks (i.e., 450 and 550 nm) appear to decay at the same rate, have been observed before, and have been assigned to the singlet.⁸ The singlet **I** yields heterolysis of the C–O bond in CH_2Cl_2 and CH_3CN , which are capable of solvating the resulting ions. The cation has been photochemically generated previously, and the assignment of the transient to the cation has been corroborated by its independent preparation.¹⁸ The lifetime of the singlet (i.e., the peaks at 450 and 550 nm) decreases as this new pathway is introduced in polar solvents. In addition, because the pair of ions results from this bond fragmentation, one must necessarily enter the $\text{S}_{\text{N}}1$ mechanism at the point of contact ion pairs (form **III**, above). Because

contact ion pairs are formed at some time shortly after fragmentation, **III** must give rise to the other kinetic forms of the ions (i.e., **IV** or **V**), and microscopic reversibility (i.e., the combination of constituent ions in **III**) allows some comment on the thermal bond breaking step, the usual rate determining step in $\text{S}_{\text{N}}1$.

Trying to assign kinetic forms from a single set of visible absorption spectra is not the goal here. However, some valuable qualitative information is available. The decay of the absorbance at 590 nm in the picosecond experiments does not appear to fit a single exponential, and there are not sufficient data to justify a fit to two or three exponentials. The absence of a single decay suggests that more than one kinetic form can be invoked. Indeed, the diffusion apart of the constituents of the contact ion pair would be expected to occur with rates in the range 10^7 – 10^8 s^{-1} that would put such an event (i.e., formation of **IV** and/or **V**) in the time frame of 0.5–10 ns.^{9b} The decay of the peak at 590 nm in methylene chloride appears to be faster than in acetonitrile and leaves a smaller amount of cation persisting into the nanosecond time scale (see Figure 2B). We also observe this in the nanosecond experiment; at ca. 20–50 ns, the absorbance at 590 nm in CH_2Cl_2 is a factor of 4–10 times less than that observed in CH_3CN under identical conditions even though the picosecond data suggest that comparable amounts are formed initially. The picosecond decays in CH_3CN (or in CH_3OH or in mixtures of the two, not shown) appear to be very similar. That the results in CH_3OH are similar to those in CH_3CN suggests that methanol has a minor role as a nucleophile or in hydrogen bonding with acetate through much of the picosecond stage.

These observations are all consistent with contact ion pairs **III** being formed early on this time scale and being the dominant form throughout much of it. Thus, methanol does not react with the cation (or interact with OAc^-), while **2** and acetate are a contact ion pair. Additional support comes from the spectra in the moderately polar solvent CH_2Cl_2 , which does not solvate the ion pair sufficiently to allow much of **IV** or **V** to form and which has little bulk stabilizing effect on the ion pair itself. Furthermore, in that solvent a small amount of **2** (compared to **2** formed in CH_3CN or DMSO under the same conditions) persists at the earliest times of the nanosecond experiment. The observed recombination rate of **2** and OAc^- in the nanosecond experiments is faster in CH_2Cl_2 than in the more polar solvents.²³

(22) A second solvent separated ion pair form in which there are two solvents between the ions has been invoked: (a) Eigen, M. *Discuss. Faraday Soc.* 1957, 24, 25. (b) Atkinson, G.; Kor, S. K. *J. Phys. Chem.* 1967, 71, 673.

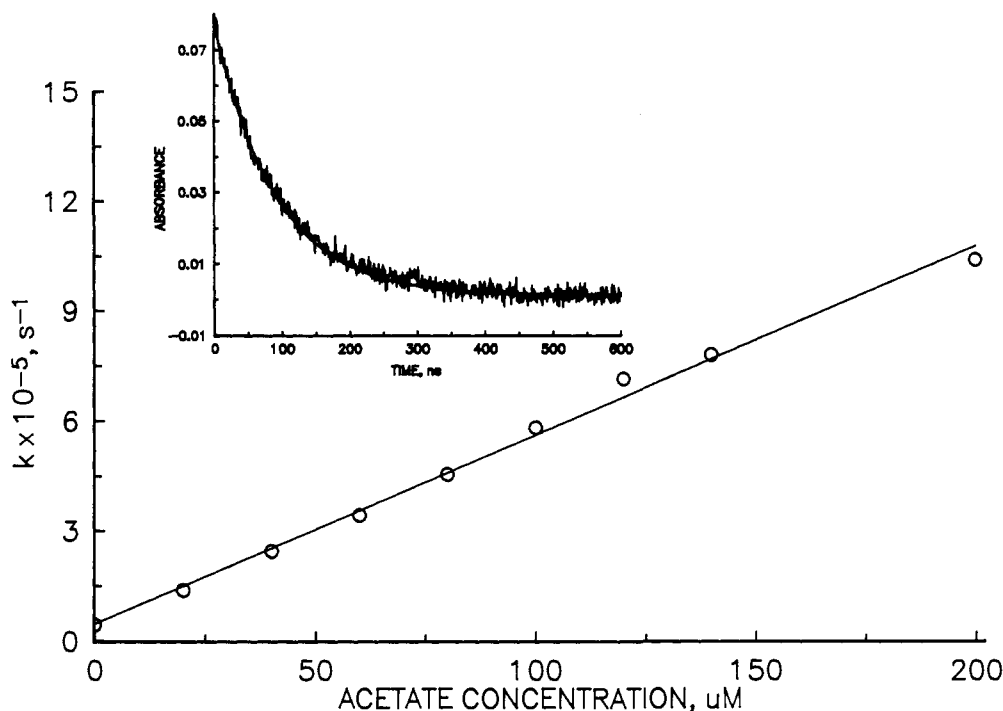


Figure 7. Observed rate from the irradiation of **1** in CH_3CN versus the concentration of acetate. The linear fit line corresponds to a second order rate constant of $5.1 \times 10^9 \text{ M}^{-1} \text{ s}^{-1}$. The inset is the actual decay of **2** at 590 nm from irradiation of **1** in CH_3CN with $200 \mu\text{M OAc}^-$, and the corresponding fit line is for the rate $1.1 \times 10^6 \text{ s}^{-1}$.

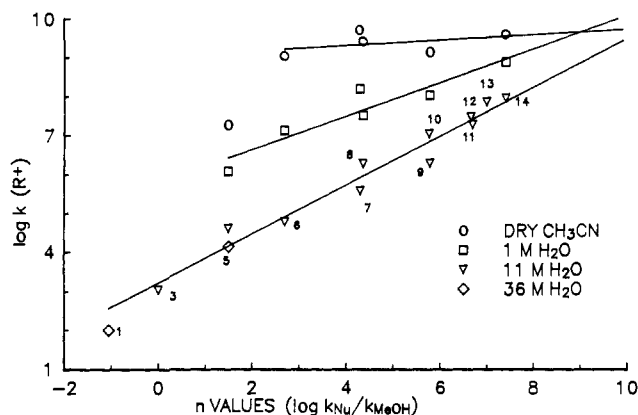


Figure 8. Plot of the log of the second order rate constants for reaction of **2** with nucleophiles (from Table I) versus the corresponding Pearson/Swain-Scott n values in the indicated solvents. The number next to the triangles identify the nucleophiles by their entry in Table I.

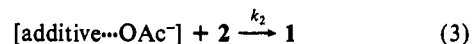
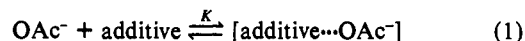
The kinetic forms **IV** and **V** may be more important at later times (i.e., $> \text{ca. } 0.5 \text{ nsec}$) in the picosecond experiments. Indirect evidence comes from changes in the peak widths or maxima especially evident at times from ca. 2–9 ns in Figure 2. Such a narrowing of the peak width or change in its maximum is similar to such phenomena observed for radical ion pairs.^{21c,24a-d} (Hydrogen bonding has been suggested^{24e} as an alternative to some of the ion pairing effects.^{21c,24a-d}) Of course, this only signals that there is some change in the present case and not what the nature of it is. Alternatively, the change in peak shape or location could be due to *trans* \rightarrow *cis* isomerization in **2** as the all-*trans* form is

converted to other geometrical isomers. Additional work will be necessary to elucidate the details of these ion dynamics at early times, but our qualitative picture is consistent with rates involving ion pairing in previous studies.⁹

One would expect that the formation of free ions in polar solvents like CH_3CN would be complete by the earliest detection times in the nanosecond experiments (ca. 20–50 ns),^{9b} and we find that such is the case here. Thus, irradiation of **1** in the nanosecond experiment leads to the absorbance at 590 nm, which clearly decays by second order kinetics. Heterolysis of **1** produces 1 equiv of each, cation **2** and acetate. The cation **2** must be in form **V** in order to react by a second order rate ($[\text{2}] = [\text{OAc}^-] = \text{ca. } 20 \mu\text{M}$).

Hydrogen Bonding and Special Salt Effects on the Leaving Group. Given that the species reacting in the Stern-Volmer studies is **IV** or **V** (or both but not **III**), we can analyze the negative, nonlinear effects of water, the alcohols, and lithium ion (Figures 4–6). In addition to the negative Stern-Volmer regions, evidence that water and the alcohols are not behaving as nucleophiles comes from the decay of cation **2** which remains second order even though the hydroxylic solvent concentration becomes quite high (ca. molar) compared to the amount of **2** (ca. $20 \mu\text{M}$). Our interpretation is quite simple; the hydroxylic solvents hydrogen bond to acetate and inhibit the recombination reaction with the less nucleophilic complex $[\text{HOH} \cdots \text{OAc}^-]$. The lithium ion behaves like a Lewis acid, complexes the acetate, and reduces its activity (i.e., nucleophilicity).

Consider the equilibrium between acetate and the hydroxylic solvent or lithium ion in the following scheme (where additive = hydroxylic solvent or lithium ion):



If $k_1 \gg k_2$, then the ratio of observed rates in the absence (k_0) and presence of additive (k_{add}) is given by

$$\frac{k_{\text{add}}}{k_0} = 1 - \frac{[\text{additive}]}{(1/K) + [\text{additive}]} \quad (4)$$

(23) The decay of **2** fits a second order rate and gives the following constants in dry solvents: CH_2Cl_2 , $5.1 \times 10^6 \text{ M}^{-1} \text{ s}^{-1} \text{ e}^{-1}$; CH_3CN , $6.3 \times 10^5 \text{ M}^{-1} \text{ s}^{-1} \text{ e}^{-1}$. (These give the true second order rates when multiplied by the extinction coefficient at 590 nm. Highly accurate values are not currently available for the first solvent.) In addition, part of the difference may be due to different diffusion controlled limits in both of these solvents.

(24) (a) Simon, J. D.; Peters, K. S. *J. Am. Chem. Soc.* **1983**, *105*, 4875–82. (b) *J. Am. Chem. Soc.* **1982**, *104*, 6142–4. (c) *J. Am. Chem. Soc.* **1982**, *104*, 6542–7. (d) *J. Am. Chem. Soc. J. Phys. Chem.* **1983**, *87*, 4855–7. (e) Fessenden, R. W.; Devadoss, C. *J. Am. Chem. Soc.* **1990**, *94*, 4540–9.

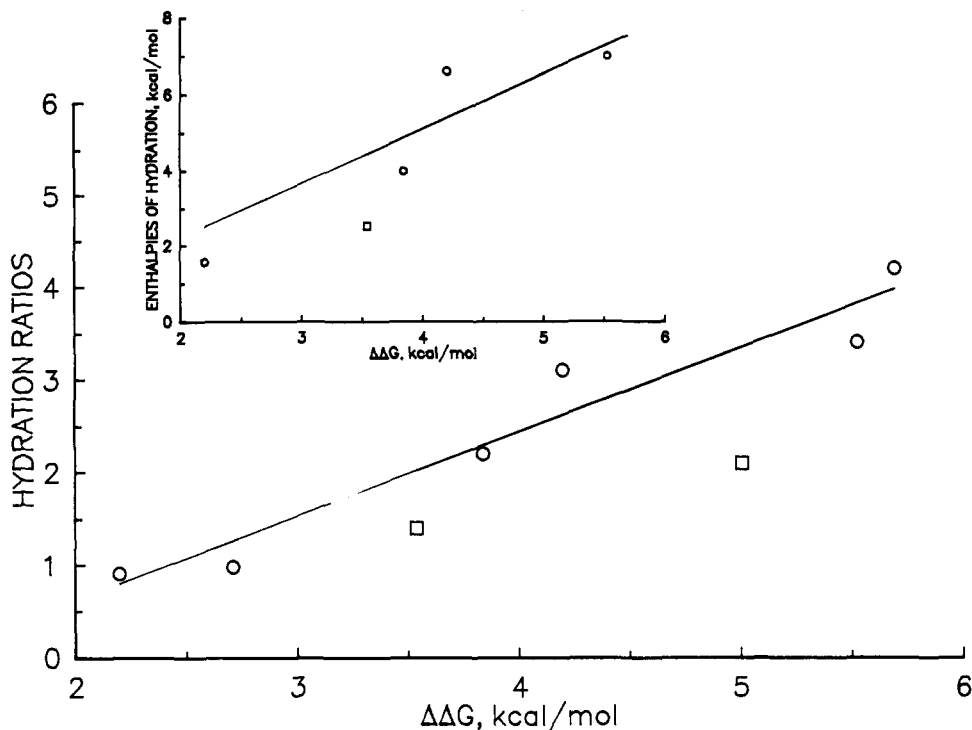


Figure 9. Hydration ratios H versus the activation energies $\Delta\Delta G^*$ for the differences in rates in dry CH_3CN and 11 M water. The inset is the total enthalpy for hydrogen bonding versus $\Delta\Delta G^*$ (see Discussion). The lines are least squares fits to the data (circles) excluding nitrate and aryl sulfonates (boxes), and the equations to them are given in the text.

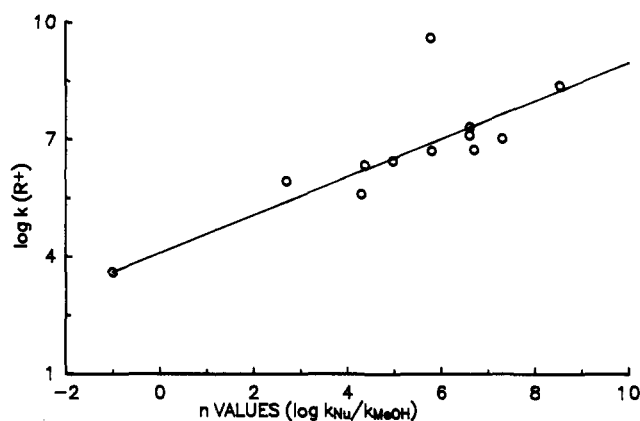


Figure 10. Plot of the log of the second order rate constants for reaction of **2** with nucleophiles versus the corresponding Pearson/Swain-Scott n values in 36 M H_2O in CH_3CN . The data and parameters for the fit line are given in ref 36.

where K is the equilibrium constant controlling the complexation of the additive

$$K = \frac{[\text{additive}\cdots\text{OAc}^-]}{[\text{OAc}^-][\text{additive}]} \quad (5)$$

One can determine the equilibrium constant K from the data used to make the plots in Figures 4–6, and those values are found to be water, 25; methanol, 25; trifluoroethanol, 250; Li^+ , 38 000.²⁵

This interpretation is consistent with other information that we have. For example, if one rearranges the equilibrium expression from eq 5 to $[\text{additive}\cdots\text{OAc}^-][\text{OAc}^-] = K[\text{additive}]$, one can look at the ratio of acetate forms in solution at various water concentrations. This is important since we would like to have only one form of the nucleophile (or in this case one form of the leaving

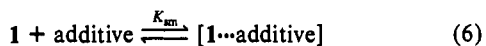
group) at a time. We can see why only one decay is observed under the conditions employed (i.e., dry CH_3CN vs 1 M H_2O). Even if there is considerable water in “dry” CH_3CN (e.g., $[\text{H}_2\text{O}] < 1 \text{ mM}$, $K = 25$), the ratio $[\text{HOH}\cdots\text{OAc}^-]/[\text{OAc}^-] = 0.025$, or in other words, less than 3% OAc^- is complexed. In contrast, at $[\text{H}_2\text{O}] = 1 \text{ M}$, $[\text{HOH}\cdots\text{OAc}^-]/[\text{OAc}^-] = 25$ and >95% of the OAc^- is hydrogen bonded. Thus, in dry CH_3CN the rates we measure will be for the uncomplexed acetate, while at 1 M water the equilibrium has shifted primarily to the hydrogen bonded form. That rate changes from 5.1×10^9 to $1.6 \times 10^8 \text{ M}^{-1} \text{ s}^{-1}$, a decrease of a factor of 32, which corroborates the assumption above that $k_1 \gg k_2$.

The effect is even more striking with Li^+ . The very large K value insures that the curve approaches the asymptotic straight line (see Figure 6) in the micromolar range. Thus, by using the relationship $[\text{Li}^+\cdots\text{OAc}^-]/[\text{OAc}^-] = 3.8 \times 10^4 [\text{Li}^+]$, the ratio of complexed to uncomplexed acetate is calculated to be ca. 10 when $[\text{Li}^+] = 300 \mu\text{M}$. In other words, OAc^- is greater than 90% complexed at concentrations of $\text{Li}^+ > 300 \mu\text{M}$, a concentration only ca. 10 times greater than that at which the cation was originally produced by the laser flash.

Because photolysis creates such a small concentration of acetate (i.e., ca. $20 \mu\text{M}$), it seems possible that the data in Figures 4 and 5 for water and the alcohols are not their first equilibria. For example, the equilibrium constant of ca. 25 for acetate and water could actually represent the second or third water being complexed. This would simply require that our dry CH_3CN contain residual water at concentrations greater than $20 \mu\text{M}$ and that the first equilibrium constant be quite large (perhaps as big as the one from lithium ion). Even if this is true, it serves no useful purpose to try to remove the last amounts of water because the rate we observe in dry CH_3CN is already at or near the diffusion controlled limit. In other words, if we could make ultradry CH_3CN solutions of **1**, we would not see any effect on the rate constant since we cannot observe a faster one. Although we cannot show unequivocally that our K values are for the first equilibrium, the data in Figures 4 and 5 suggest that they are and serve to demonstrate that water and the alcohols play a critical role in $\text{S}_{\text{N}}1$ reactions by determining the rate of recombination of the cation and leaving group. Likewise, reaction rate attenuation by cosolvent hydrogen bonding will be demonstrated for the series of nucleophiles used.

(25) These values for K were determined by minimizing the difference between the observed k_{add}/k_0 values (data in Figures 4–6) and ones calculated from the equations above. That we have approached the correct values is obvious in the best fit lines that have been drawn in the figures.

Another question concerns the consequences, if any, of the interaction between the "additive" (i.e., H₂O, ROH, Li⁺) and the precursor **1**. One would expect that the equilibrium constant K_{sm}



would be smaller than K in eq 1 (e.g., $K_{sm} \ll 25$ for water) simply based on the structures of acetate and **1**. Furthermore, irradiation of [1...additive] would lead to an ion pair [2, AcO⁻...additive] in which acetate is hydrogen bonded and whose recombination would be inhibited. Such an inhibition should lead to an increase in the concentration of **2** (i.e., absorbance at 590 nm) at the earliest times in the nanosecond experiment (i.e., the initial OD) as a function of [H₂O]. This was not observed, since the initial OD is constant over the range [H₂O] = 0–2 M. The ratio of [1...H₂O]/[1] is given by $K_{sm}[\text{H}_2\text{O}]$. If one assumes the ratio [1...H₂O]/[1] < 0.1 (i.e., we would observe a 10% change) for [H₂O] = 2 M, then $K_{sm} < 0.05$. (In fact, K_{sm} must be smaller than that value because the picosecond spectra in MeOH are very similar to those in CH₃CN.)

The reactions of water and the alcohols as nucleophiles can be seen in Figures 4 and 5 at the higher concentrations of the hydroxylic cosolvent. The slope of the linear portion of the plot for water, and thus the second order rate constant for the reaction of **2** with water (as a nucleophile), is sufficiently small that it is difficult to ascertain accurately. Figure 4 shows the recombination of **2** with OAc⁻ that is dominated by the hydrogen bonding equilibrium at low concentrations as the figure in the inset (with second order rate constants as the ordinate) but shows the reaction with water at higher concentrations with the first order rate constants in the ordinate at the bottom of the main figure (dashed line).

Methanol and isopropyl alcohol have sufficiently larger second order rates, and the positive Stern–Volmer regions are quite obvious. In fact, the latter two are either markedly curved or appear to have two linear regions. (The highest concentrations of methanol and 2-propanol in the plot are actually neat alcohol.) The nature of the Stern–Volmer data suggests that the nucleophilicity of the alcohol depends on the nature of the bulk solvent.

The presence of distinct regions for the interaction of water or alcohols with cation **2** and others^{26,27} suggests a caveat concerning data in the literature. *Comparison of rates from reactions under different conditions or attempts to interconvert data may be quite unpredictable.* This warning has also been voiced recently by McClelland et al.^{1a} Fortunately, most solvolyses have been conducted at relatively high water concentrations (20% aqueous solutions or ca. 11 M H₂O are common). This corresponds to the flat or asymptotic portion of the equilibrium where small changes in water content may not have any meaningful effect of the rate. However, it is quite likely that with anions that are stronger hydrogen bond acceptors than OAc⁻, two or three hydroxylic solvents may hydrogen bond to each anion, and an additional diminution of nucleophilicity may be observed.

Relative Nucleophilicity and Selectivity. Absolute rate constants for the reaction of a variety of nucleophiles with **2** are listed in Table I and plotted in Figure 8 as a function of the water content of the CH₃CN solutions. The three lines in Figure 8 tell the whole story. The slope of each line is a measure of nucleophile selectivity of the cation **2**. The selectivity increases with added water and apparently reaches a limiting value. Water has a profound effect on the less reactive of the nucleophiles as defined by Pearson's n values; fluoride rate change by four orders of magnitude in going from CH₃CN to 11 M H₂O in CH₃CN. At the other extreme, iodide changes only by a factor of ca. 40.²⁶

(26) Similar rate data can be used to demonstrate the effect of Li⁺. For example, we have measured rates in 10 mM Li⁺ClO₄⁻ in dry CH₃CN, and they appear to give rates that parallel the hydrogen bonding ones in 11 M water.

(27) The specific interactions between hydroxylic solvents or cations like Li⁺ and leaving groups or nucleophiles have been observed in the presence of a variety of cations: Pienta, N. J.; Kessler, R. J. *J. Am. Chem. Soc.*, manuscript in preparation.

There are two major observations of note in Figure 8: (1) the linear correlation of log k (the rate for cation combination with nucleophiles) with n values (S_N2 rates) and (2) the origin in the change of rates with water content (i.e., different slopes of the lines). The marked change in rate of recombination of OAc⁻ with **2** and the rate changes in the nucleophilicities in Table I must arise from the same phenomenon, hydrogen bonding to the cosolvent water. Besides the equilibria in Figures 4 and 5, other direct evidence comes from some calorimetric data of Arnett, Chawla, and Hornung²⁸ and, in general, is supported by studies on anion hydration.²⁹ Arnett et al. measured the heats evolved when various anions (as the TBA salts in solution in dry nitrobenzene) were introduced into water-saturated nitrobenzene. Thus, the enthalpies are a measure of the total hydrogen bonding, resulting from as many water molecules as become complexed to the anion when millimolar solutions of it are added to ca. 0.17 M water in nitrobenzene. The data are as follows (anion, enthalpy in kcal/mol): acetate, 7.0; chloride, 6.6; bromide, 4.0; nitrate, 2.5; and iodide, 1.57. Furthermore, Arnett et al. determined hydration ratios H (defined as the number of moles of water to the number of moles of salt at equilibrium in nitrobenzene), and some representative values are as follows (anion, H): fluoride, 4.2; acetate, 4.0; chloride, 3.1; bromide, 2.2; phenyl sulfonate, 2.1; nitrate, 1.4; thiocyanate, 0.98; iodide, 0.91; triflate, 0.55. Both of these sets of calorimetric data can be compared with $\Delta\Delta G^\ddagger$ calculated from the rate data in Table I. Thus, we can use reaction rate theory³¹ to predict what increases in $\Delta\Delta G^\ddagger$ must accompany the rate change observed in going from dry CH₃CN to 11 M water. The results are shown as $\Delta\Delta G^\ddagger$ in Table I. Figure 9 is a plot of the Arnett hydration numbers versus $\Delta\Delta G^\ddagger$ from the rate data, while the inset to that figure is a plot of the total hydrogen bonding enthalpies (vide infra) versus $\Delta\Delta G^\ddagger$. There is a direct relationship between the enthalpic values obtained by Arnett and the energy term determined from the ratios of rates: total hydrogen bonding enthalpy = $0.91 \Delta\Delta G^\ddagger - 1.2$, $r^2 = 0.97$ for six values; hydration ratio $H = 1.44 \Delta\Delta G^\ddagger - 0.66$, $r^2 = 0.94$ for four values. The anions that are exceptional (nitrate, triflate, phenyl sulfonate) are nucleophiles that have the lowest n values and, in cases where we were able to measure them, had second order rates (in Table I) considerably below diffusion control in dry CH₃CN.

As we move from right to left along the abscissa in Figure 8, the strength of the hydrogen bonding increases (up to fluoride, at least) and has two consequences of importance here. First, the nucleophilic electron pair becomes less available to the electrophilic cation, and, second, the magnitude of the equilibrium constant increases. Each of these factors can independently account for the observations. It is likely that both are in effect. A very large equilibrium constant for complexation of the first water increases the likelihood that a second molecule and additional water molecules may become complexed. An anion hydrogen bonded to multiple molecules of water will suffer from reduced reactivity from the diminished availability of the lone pair both electronically (i.e., reduced charge density) and spatially (i.e., prevention of orbital overlap). The rate diminution on going from dry CH₃CN to 1 M water has been shown to be due to the complexation of a single water to acetate. The rate decrease on going from 1 to 11 M water is likely to involve more molecules of hydrogen

(28) Arnett, E. M.; Chawla, B.; Hornung, N. J. *J. Solution Chem.* 1977, 6, 781–818.

(29) (a) Mohr, S. C.; Wilk, W. D.; Barrow, G. M. *J. Am. Chem. Soc.* 1965, 87, 3048. (b) Benoit, R. L.; Lam, S. Y. *J. Am. Chem. Soc.* 1976, 96, 7385. (c) Benoit, R. L.; Buisson, C. *Inorg. Chim. Acta* 1973, 7, 256. (d) Choux, G.; Benoit, R. L. *J. Am. Chem. Soc.* 1969, 91, 6221. (e) Kenjo, T.; Diamond, R. M. *J. Inorg. Nucl. Chem.* 1974, 36, 183. (f) Kenjo, T.; Diamond, R. M. *J. Phys. Chem.* 1972, 76, 2454. (g) Cogley, D. R.; Butler, J. N.; Grunwald, E. *J. Phys. Chem.* 1971, 75, 1477. (h) Kolthoff, I. M. *Anal. Chem.* 1974, 46, 1992. Kuntz, I. D., Jr.; Cheng, C. J. *J. Am. Chem. Soc.* 1975, 97, 4852 and references cited therein.

(30) Lowry, T. H.; Richardson, K. S. *Mechanism and Theory in Organic Chemistry*, 3rd ed.; Harper & Row: New York, 1987; pp 369–70.

(31) Reaction rate theory predicts that the change in activation barrier $E_a = RT \ln k_1/k_2$ or $1.34 \log k_1/k_2$ at 22 °C. See ref 30, pp 210–11.

bonding solvent, and it is tempting to speculate that Arnett's hydration ratios H supply the stoichiometry. That analysis awaits more data (e.g., anion hydrogen bonding enthalpies in CH_3CN), and additional discussion will follow.²⁷

The other significant observation in Figure 8 is the linear correlation between the rates for cation and nucleophile combination and the n values,¹⁷ a scale derived from and based on $\text{S}_{\text{N}}2$ rates. One would expect steric factors to be present in the n values, although the use of iodomethane as the model substrate may minimize this potential problem. On the other hand, $\text{S}_{\text{N}}1$ values involve a carbon center with a full positive charge. The success of the correlations in Figure 8 and similar ones for other cations below and elsewhere²⁷ is testimony to its utility in this regard. (Attempts to use the pK_{a} of the conjugate acid of the nucleophile³¹ or the redox potential for nucleophile oxidation,³⁴ alternatively suggested measures of nucleophilicity, were unsuccessful; they produced scatter plots.)

The relationships in Figures 8 and 9 suggest that Pearson's n values are inversely related to the strength of the nucleophile's ability to hydrogen bond. Indeed, the n values were determined in CH_3OH as solvent, and an inverse relationship between n values and hydration ratios H was reported by Arnett et al.²⁹ We suggest that the n scale is made up of two groups of nucleophiles: (1) those whose reactivity is dominated by hydrogen bonding ($n \geq \text{ca. } 2.5$) in appropriate mixed solvents and (2) those controlled by a small hydrogen bonding effect in addition to a diminished reactivity that results from their structure. We include nitrate and the aryl sulfonates (i.e., tosylate, triflate, phenyl sulfonate) in the latter group. In other words, nitrate and the aryl sulfonates have low n values because they are inherently poor nucleophiles even in the absence of hydrogen bonding solvents and are made even less nucleophilic in their presence. In principle, the rates of cation-nucleophile combination and $\text{S}_{\text{N}}2$ rates should not correlate in acetonitrile since we claim the effect is due to hydrogen bonding in both cases. In fact, the fit of the uppermost line in Figure 8 is only good for the points corresponding to rates at or near the diffusion controlled limit. (In such a case, the use of any values on the abscissa will give a straight line with zero slope!) As a result, the comparison of rates of cation-nucleophile combination and $\text{S}_{\text{N}}2$ rates in non-hydrogen bonding solvents is being pursued and will be reported separately. Nonetheless, these two reactivities are highly correlated in mixed solvents with hydroxylic components.

The slopes of the lines in Figure 8 are equivalent to the selectivity measure, $\log k_{\text{azide}}/k_{\text{water}}$, that has become quite popular in the literature.^{4,30,32-35} The slopes in Figure 8 (CH_3CN , 0.007; 1 M H_2O , 0.43; 11 M H_2O , 0.63) can be converted to these ratios simply by multiplying the slope by 6.8, the difference between the n values of azide (5.78) and water (-1.05). Our values (i.e., the slopes of the lines from plots like those in Figure 8) are inherently more dependable since we use more than two values. The $\log k_{\text{azide}}/k_{\text{water}}$ values calculated from the data here are for dry CH_3CN , ca. 0.05; for 1 M H_2O in CH_3CN , ca. 2.9; and for 11 M H_2O in CH_3CN , ca. 4.2. The last one would be most comparable to conditions under which others in the literature were generated.

We offer a warning concerning the use of $\log k_{\text{azide}}/k_{\text{water}}$ ratios as selectivity measures. We do not favor the use of either component that makes up the ratio as the result of some observations. The first potential problem lies in the conversion of the observed first order rate (from the reaction with water) into a second order rate; simply dividing by the solution water concentration may not be appropriate if one considers the data in Figures 4 and 5. Furthermore, we have observed that reported rate constants from

some groups (vide supra) for reactions of various cations with azide are systematically high (when compared to a value predicted by plots of $\log k$ vs n values).

A General Model. All that remains to be demonstrated is whether cation **2** is a typical carbenium ion. Are the phenomena demonstrated here general to the whole class of intermediates and what are the expected consequences? The effects that we have demonstrated have all been due to the leaving group and the nucleophiles. A priori we would expect them to be observed for other cations and find that that is the case for every example we have investigated (including triarylmethyl, xanthylium, benzhydryl, tropylium, and phenethyl cations).²⁷ For example, a plot of the rate data for combination of the triphenylmethyl (trityl) cation with nucleophiles versus n values uses the data of McClelland et al.^{1c,36} and is shown in Figure 10. These data also produce an excellent fit to a straight line (with the exception of the point for azide).³⁶

We can also make the case for the retinyl cation being a typical cation in another way. A current model for reactions of cations and nucleophiles tries to relate reactivity (\log of the solvolysis rate of the alkyl or arylalkyl chloride in 20% aqueous acetone) and selectivity ($\log k_{\text{azide}}/k_{\text{water}}$).⁴ Four regions were originally defined, although recent work suggests that two may not be different at all.^{1a} Nonetheless, we present the original model (although not adhering to the original numbering of the regions): (1) a region (fastest solvolyses and largest selectivities) with constant selectivity (i.e., the N_+ values), suggested to account for the stable cations studied by Ritchie;² (2) a region containing mostly alkyl and some resonance stabilized cations, suggested to obey the reactivity-selectivity principle by Raber, Harris, Hall, and Schleyer;³³ (3) a region (slowest solvolysis and smallest selectivities) that has been suggested by Jencks and Richard to account for arylalkyl cations reacting via competing $\text{S}_{\text{N}}1$ and $\text{S}_{\text{N}}2$ mechanisms that depend on the solvent and substrates.^{7,34}

Cation **2** can be placed in region 2 in the model above using the selectivity determined above ($\log k_{\text{azide}}/k_{\text{water}} = 4.2$ in 11 M H_2O , determined from the slope in Figure 8) and a solvolysis rate constant measured in this study ($\log k_{\text{sol}} = -1.5$). The reaction of **1** in 20% aqueous acetone at 70 °C occurred with a rate constant of $2.3 \times 10^{-5} \text{ s}^{-1}$ and was converted to a rate of $4.6 \times 10^{-8} \text{ s}^{-1}$ at 25 °C. Acetates react 1.4×10^{-6} times as fast as chlorides.³⁴ This predicts a rate for retinyl chloride at 25 °C in 20% aqueous acetone as $3.3 \times 10^{-2} \text{ s}^{-1}$ ($\log k = \text{ca. } -1.5$). (We feel justified in making the acetate/chloride correction in spite of our own earlier warnings since those two anions have the same n values and thus, similar hydrogen bonding capacity according to our suggestions.) This places cation **2** in the middle of region 2, an ideal location for a "typical" or model cation.

Conclusions

Irradiation of retinyl acetate **1** leads to formation of the retinyl cation **2** within hundreds of picoseconds and affords the opportunity to study subsequent combination reactions with nucleophiles as a model for those aspects of the $\text{S}_{\text{N}}1$ reaction. We suggest evidence for the contact ion pairs in times after the generation of **2** and before the appearance of free ions early in the nanosecond experiment. Free ions of cation **2** undergo recombination with the leaving group, acetate, that reacts at rates greatly diminished in the presence of hydroxylic solvents or lithium ions. Equilibrium constants for the hydrogen bonds between OAc^- and the cosolvents were measured, as were the rates of nucleophiles complexed or uncomplexed to water. The amount of water gives rise to different relative reactivities for a variety of nucleophiles, and those rates can be correlated to Pearson's n values, measures of relative reactivity for the nucleophiles by an $\text{S}_{\text{N}}2$ mechanism. This be-

(32) Wayner, D. D. M. In *Handbook of Organic Photochemistry*; Scaiano, J. C., Ed.; CRC Press: Boca Raton, FL, 1989; Vol. II, p 363-8.

(33) Raber, D. J.; Harris, J. M.; Hall, R. E.; Schleyer, P. v. R. *J. Am. Chem. Soc.* **1971**, *93*, 4821-8.

(34) Richard, J. P.; Jencks, W. P. *J. Am. Chem. Soc.* **1982**, *104*, 4689-91 and 4691-2.

(35) (a) Noyce, D. S.; Virgilio, J. A. *J. Org. Chem.* **1972**, *37*, 2643. (b) Stang, P. J.; Hanack, M.; Subramanian, L. R. *Synthesis* **1982**, 85-126.

(36) Reference 1c contains rate constants for the reactions of more than 20 nucleophiles with triphenylmethyl cation generated by laser flash photolysis in 36 M water in acetonitrile. The rates for which n values are available were used in the plot and are as follows (nucleophile, $\log k$): water, 3.61; fluoride, 5.93; acetate, 5.60; chloride, 6.34; imidazole, 6.45; azide, 9.61; bromide, 6.70; hydroxylamine, 7.11; hydrazine, 7.32; cyanide, 6.74; piperidine, 7.02; sulfite, 8.38. The slope of the least squares line is 0.487, and the y -intercept is 4.01.

havior is believed to be general for this class of intermediates.

Acknowledgment. We are grateful to Kevin Peters and Erin O'Driscoll (University of Colorado) for their help in obtaining the picosecond spectra, to the University of Arkansas for a sabbatical leave, and to T. J. Meyer (University of North Carolina) for the use of his nanosecond equipment. We thank E. M. Arnett (Duke University) and R. A. McClelland (Toronto) for their thoughtful comments and suggestions. We appreciate the com-

ments of a referee who made a number of valuable suggestions concerning our picosecond data.

Registry No. 1, 127-47-9; 2, 20056-09-1; Li^+BF_4^- , 14283-07-9; $\text{Li}^+\text{ClO}_4^-$, 7791-03-9; $\text{TBA}^+\text{BF}_4^-$, 429-42-5; Li^+ , 17341-24-1.

Supplementary Material Available: A derivation of eq 4 (2 pages). Ordering information is given on any current masthead page.

Characterization of Thiol Self-Assembled Films by Laser Desorption Fourier Transform Mass Spectrometry

Yunzhi Li, Jingyu Huang, Robert T. McIver, Jr.,* and John C. Hemminger*

Contribution from the Department of Chemistry and Institute for Surface and Interface Science, University of California, Irvine, Irvine, California 92717. Received July 18, 1991

Abstract: Self-assembled alkanethiol monolayers on gold films have been studied using the technique of laser desorption coupled with Fourier transform mass spectrometry. We demonstrate that thiol molecules can be desorbed intact using 193-nm laser radiation. Information on the self-assembled films at a molecular level is achieved. In addition to the well-known thiolate species, alkane sulfonates resulting from air exposure of the self-assembled film are also detected. No phase segregation ≥ 30 μm is observed from the laser desorption of self-assembled films made of alkanethiol mixtures.

Introduction

Self-assembled monolayer films have recently been the subject of intense study. The self-assembled films that have been studied most are the self-assembled thiol or disulfide on a gold surface with the techniques of infrared spectroscopy (IR), X-ray photoelectron spectroscopy (XPS), high-resolution electron energy loss spectroscopy (HREELS), temperature-programmed desorption (TPD), wetting chemistry, optical ellipsometry, electrochemistry, electron diffraction, He diffraction, $^3\text{He}^+$ diffraction, X-ray diffraction, and scanning tunneling microscopy.¹⁻³³ The XPS

data indicate that monolayers of thiols are formed on gold surfaces. The ellipsometry and IR measurements indicate that the hydrocarbon chain of the thiol is tilted away from the perpendicular to the gold surface. The He and electron diffraction experiments show that the hydrocarbon chains are ordered and that less ordered films are formed as the carbon chain length decreases. Electrochemistry studies exhibit no pinholes in the films. On the basis of these studies, a picture has emerged in which a well-ordered monolayer of thiolate covers the Au surface such that all sulfur atoms are bonded to Au with the carbon chain uniformly oriented at a tilt angle from the surface normal. A variety of self-assembled films have been studied using the different techniques described above, but information on the molecular composition of the films is obtained from indirect observations. For example, more direct evidence is required to definitively conclude whether thiolates or thiols are formed on the self-assembled films, and little is known about molecular impurities.

- (1) Nuzzo, R. G.; Allara, D. L. *J. Am. Chem. Soc.* **1983**, *105*, 4481-4483.
- (2) Nuzzo, R. G.; Zegarski, B. R.; Dubois, L. H. *J. Am. Chem. Soc.* **1987**, *109*, 733-740.
- (3) Nuzzo, R. G.; Fusco, F. A.; Allara, D. L. *J. Am. Chem. Soc.* **1987**, *109*, 2358-2368.
- (4) Porter, M. D.; Bright, T. B.; Allara, D. L.; Chidsey, C. E. D. *J. Am. Chem. Soc.* **1987**, *109*, 3559-3568.
- (5) Dubois, L. H.; Zegarski, B. R.; Nuzzo, R. G. *Proc. Natl. Acad. Sci. U.S.A.* **1987**, *84*, 4739-4742.
- (6) Finklea, H. O.; Avery, S.; Lynch, M.; Furttsch, T. *Langmuir* **1987**, *3*, 409-413.
- (7) Troughton, E. B.; Bain, C. D.; Whitesides, G. M.; Nuzzo, R. G.; Allara, D. L.; Porter, M. D. *Langmuir* **1988**, *4*, 365-385.
- (8) Strong, L.; Whitesides, G. M. *Langmuir* **1988**, *4*, 546-558.
- (9) Holmes-Farley, S. R.; Bain, C. D.; Whitesides, G. M. *Langmuir* **1988**, *4*, 921-937.
- (10) Bain, C. D.; Whitesides, G. M. *Angew. Chem., Int. Ed. Engl.* **1989**, *28*, 506-512.
- (11) Bain, C. D.; Biebuyck, H. A.; Whitesides, G. M. *Langmuir* **1989**, *5*, 723-727.
- (12) Bain, C. D.; Troughton, E. B.; Tao, Y.-T.; Evall, J.; Whitesides, G. M.; Nuzzo, R. G. *J. Am. Chem. Soc.* **1989**, *111*, 321-335.
- (13) Bain, C. D.; Evall, J.; Whitesides, G. M. *J. Am. Chem. Soc.* **1989**, *111*, 7155-7164.
- (14) Bain, C. D.; Whitesides, G. M. *J. Am. Chem. Soc.* **1989**, *111*, 7164-7175.
- (15) Chidsey, C. E. D.; Liu, G.-Y.; Rowntree, P.; Scoles, G. *J. Chem. Phys.* **1989**, *91*, 4421-4423.
- (16) Hautman, J.; Klein, M. L. *J. Chem. Phys.* **1989**, *91*, 4994-5001.
- (17) Whitesides, G. M.; Laibinis, P. E. *Langmuir* **1990**, *6*, 87-96.
- (18) Chidsey, C. E. D.; Loiacono, D. N. *Langmuir* **1990**, *6*, 682-691.
- (19) Stole, S. M.; Porter, M. D. *Langmuir* **1990**, *6*, 1199-1202.
- (20) Nuzzo, R. G.; Dubois, L. H.; Allara, D. L. *J. Am. Chem. Soc.* **1990**, *112*, 558-569.

- (21) Dubois, L. H.; Zegarski, B. R.; Nuzzo, R. G. *J. Am. Chem. Soc.* **1990**, *112*, 570-579.
- (22) Chidsey, C. E. D.; Bertozzi, C. R.; Putvinski, T. M.; Mujcs, A. M. *J. Am. Chem. Soc.* **1990**, *112*, 4301-4306.
- (23) Nuzzo, R. G.; Korenic, E. M.; Dubois, L. H. *J. Chem. Phys.* **1990**, *93*, 767-773.
- (24) Evans, S. D.; Ulman, A. *Chem. Phys. Lett.* **1990**, *170*, 462-466.
- (25) King, D. E.; Czanderna, A. W. *Surf. Sci.* **1990**, *235*, L329-332.
- (26) Pale-Grosdemange, C.; Simon, E. S.; Prime, K. L.; Whitesides, G. M. *J. Am. Chem. Soc.* **1991**, *113*, 12-20.
- (27) Miller, C.; Cuendet, P.; Gratzel, M. *J. Phys. Chem.* **1991**, *95*, 877-886.
- (28) Samant, M. G.; Brown, C. A.; Gordon, J. G., II *Langmuir* **1991**, *7*, 437-439.
- (29) Widrig, C. A.; Alves, C. A.; Porter, M. D. *J. Am. Chem. Soc.* **1991**, *113*, 2805-2810.
- (30) Evans, S. D.; Urankar, E.; Ulman, A.; Ferris, N. *J. Am. Chem. Soc.* **1991**, *113*, 4121-4131.
- (31) Hickman, J. J.; Ofer, D.; Laibinis, P. E.; Whitesides, G. M.; Wrigton, M. S. *Science* **1991**, *252*, 688-691.
- (32) Haussling, L.; Michel, B.; Ringsdorf, H.; Rohrer, H. *Angew. Chem., Int. Ed. Engl.* **1991**, *30*, 569-572.
- (33) Camillone, N., III; Chidsey, C. E. D.; Liu, G.-Y.; Putvinski, T. M.; Scoles, G. *J. Chem. Phys.* **1991**, *94*, 8493-8502.